

# Mixing and dynamics induced by flexible canopies composed of high-aspect-ratio structures

Lai Wing<sup>1</sup>, Liu Hong<sup>2</sup>, Leonardo P. Chamorro<sup>2,3,4\*</sup>

<sup>1</sup>TSI Incorporated, Fluid Mechanics Research Instrument, Shoreview, MN, USA

<sup>2</sup>University of Illinois at Urbana-Champaign, Department of Mechanical Science and Engineering, Urbana, IL, USA

<sup>3</sup>University of Illinois at Urbana-Champaign, Department of Civil and Environmental Engineering, Urbana, IL, USA

<sup>4</sup>University of Illinois at Urbana-Champaign, Department of Aerospace Engineering, Urbana, IL, USA

\*lpchamo@illinois.edu

## Abstract

The flow field and unsteady dynamics of a fully submerged, flexible canopy are explored experimentally under various flow conditions. The canopy is composed of thin, large-aspect-ratio, flexible structures placed in staggered patterns in a developed boundary layer. Planar and volumetric particle image velocimetry (PIV) were used to quantify the turbulence statistics in the vicinity of the canopy, whereas particle tracking velocimetry (PTV) was used to characterize the dynamics of selected plates along the center of the canopy. In the talk, we will discuss the distinctive flow-structure interaction as a function of the Reynolds and Cauchy numbers. In particular, we will discuss the motions of the structures and the distinctive modulation of the flexible structures on the turbulence dynamics.

## 1 Introduction

In general, canopies have a very large impact on the surrounding flow and far field dynamics. Understanding the dominant processes modulating the flow and canopy interaction across scales is crucial to predict a number of phenomena, including pollutant transport (Belcher 2005) and microclimate dynamics (Souch and Grimmond 2006). Aquatic vegetation plays a dominant role on the kinematics and dynamics of river flows; it modulates water waves (Fonseca and Cahalan 1992), provides habitat to a wide range of species (Hawkins et al. 1983), contributes to improve water quality (Dennison et al. 1993), and reduces the wall shear stress, among others. Turbulence over canopies exhibits distinct structure and levels that depend on the relative location, canopy layout and density, flow features as well as geometry and stiffness of the canopy elements. A comprehensive discussion on the turbulence over plant canopies can be found in Finnigan 2000.

In this study, we discuss the interaction between flow and flexible canopies with staggered patterns. Particular emphasis is placed on the unsteady motions of the canopy elements and their effect of the structure of the flow.

## 2 Experimental setup

A flexible canopy was placed in a 2.5 m long, 112.5 mm wide, recirculating flume, which was operated as open channel with subcritical flow conditions. The canopy was composed of prismatic structures casted from Silicone, which shared the same height of  $h=37.5$  mm, width  $w=6.4$  mm, and thickness  $e=2$  mm, as well as a Young's Modulus of  $E = 2.05$  MPa and density  $\rho_m= 1030$  kg m<sup>-3</sup>. The elements were distributed in a staggered pattern, with a constant spacing of  $S_x/w=1.56$  and  $S_y/w=3.125$  in the streamwise and transverse directions; see layout in figure 1. Aqueous sodium iodide solution was used as working fluid with density  $\rho_f = 1800$  kg m<sup>-3</sup> and kinematic viscosity  $\nu = 1.1 \times 10^{-6}$  m<sup>2</sup> s<sup>-1</sup>. The experiments were performed at Reynolds numbers  $Re_H = U_\infty H/\nu$ , Froude numbers  $Fr = U_\infty/(gH)^{1/2}$ , and Cauchy numbers  $Ca = \rho_f \times w \times U_\infty^2 \times h^3/(EI)$  (Luhar and Nepf) given in table 1. Here,  $U_\infty$  is the incoming freestream velocity,  $H$  is the reference water depth, and  $\nu$  is the kinematic viscosity of the fluid.

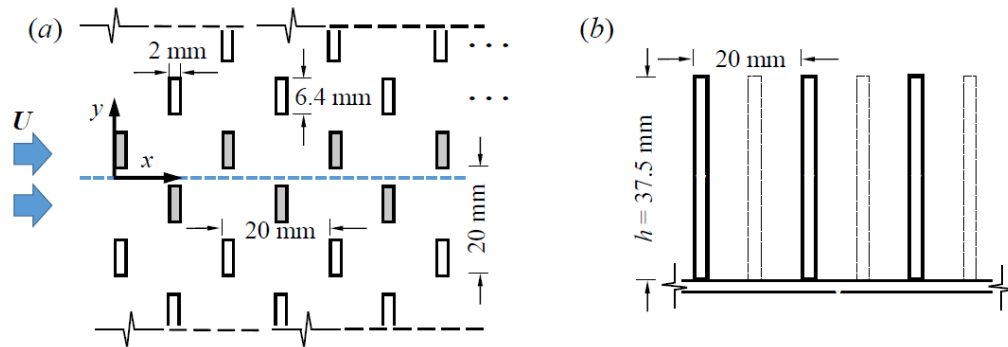


Figure 1. Basic schematics of the flexible canopy. a) Plan view of the staggered array illustrating geometry and spacing of the elements. The blue, dashed line indicates the streamwise wall-normal PIV plane at the center of the canopy; tip motions of the gray structures around the center were characterized with the PTV. b) Side view.

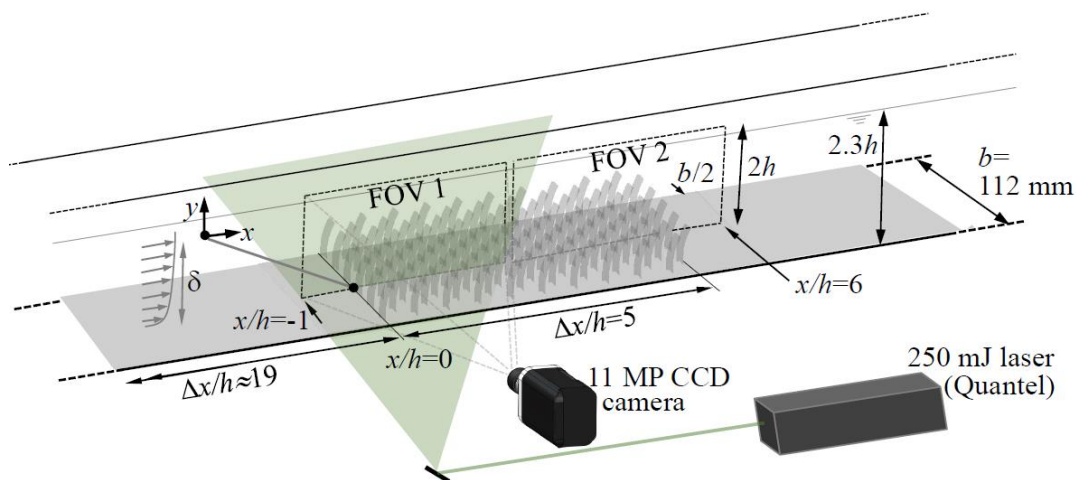


Figure 2. Schematic of the experimental set-up illustrating the general dimensions, the two streamwise, wall normal PIV measurement planes covering the flexible canopy.

$U_\infty$ (m s <sup>-1</sup> )	$Re_H$	$Fr$	$Ca$
0.18	$1.8 \times 10^4$	0.17	2.25
0.27	$2.8 \times 10^4$	0.25	5.06
0.36	$3.7 \times 10^4$	0.34	9.00

Table 1. Basic parameters setting.

Flow field measurements were conducted at two locations, which contained the span of the canopy. The flow field data was obtained in a streamwise wall normal ( $x$ - $y$ ) plane in the middle of the canopy model, as showed in dashed line in figure 1a. A planer high-resolution particle image velocimetry (PIV) system from TSI was employed for velocity field measurement of two wall-normal fields of view (FOVs). The two FOVs were illuminated by 1mm thick laser sheet generated by a 250mJ/pulse double-pulsed laser from Quantel; 14  $\mu$ m silver-coated, hollow glass spheres with density of 1700 kg m<sup>-1</sup> was chosen to seed the working fluid. For each FOV, two thousand pairs of images were collected by an 11 megapixel (4000  $\times$  2672 pixels), 12-bit, frame straddle, charge-coupled device (CCD) camera. The raw image pairs were processed by recursive cross-correlation method by using the Insight 4G software from TSI. The final interrogation window was 24  $\times$  24 pixels with 50% overlap, resulting in a vector grid spacing  $\Delta x = \Delta y = 720 \mu$ m.

The motion of the canopy elements (tips) along the center of the canopy was tracked at a frequency of 150 Hz during 60 s. The images were obtained with a Mikrotron EoSens 4CXP MC 4082 camera at 2 MP resolution. A  $6h \times 2h$  FOV was illuminated with two Stanley Lithium Ion Halogen Spotlights. The raw images were processed with a pixel to distance ratio of 0.08 mm pixel<sup>-1</sup> using the open source software OpenPTV; see details in Kim et al. 2016.

### 3 Results

In this talk, we will present and discuss distinct features of the flow statistics and structure of the turbulence induced by the flexible canopy. For the purpose, we will show insight from planar and volumetric PIV. Similarly, we will discuss the multiscale motions of the flexible elements along the center of the canopy span. We will also illustrate the impact of canopy features on the surrounding flow. Figures 3-5 show some features we will discuss during the talk. For instance, figure 3 illustrates the flow statistics around the staggered canopy at various Reynolds numbers within subcritical flow conditions, and the change of the onset of the internal shear layer with different flows. Figure 4 shows the time-averaged position of the tip elements for various flows; in particular, it shows the zone affected by the flow. Figure 5 depicts examples of the structure (spectra) of the tip motions of selected elements; they illustrate single and bi-modal features, which have distinct impact on the local flow.

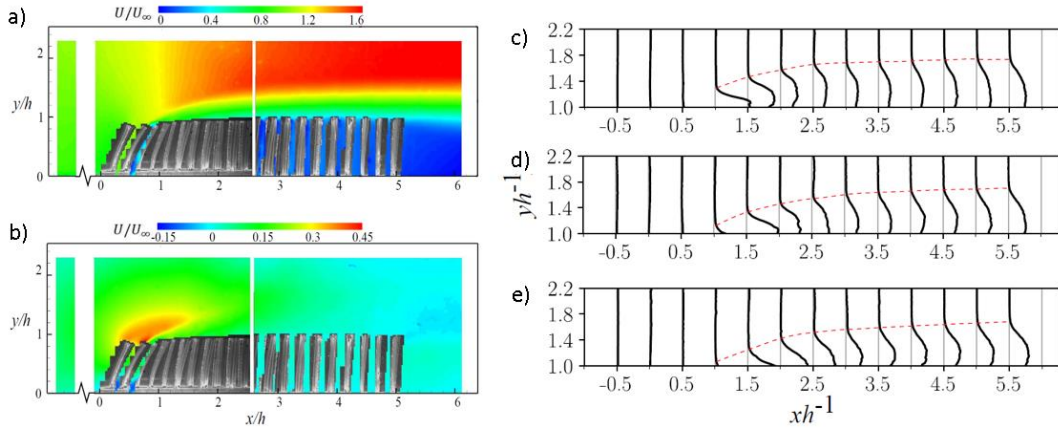


Figure 3: a) Streamwise and b) vertical velocity around a staggered, flexible canopy at  $Re=2,8 \times 10^4$ . Turbulence kinetic energy at the top of the canopy at Reynolds numbers of c)  $1,8 \times 10^4$ , d)  $2,8 \times 10^4$  and e)  $3,7 \times 10^4$ .

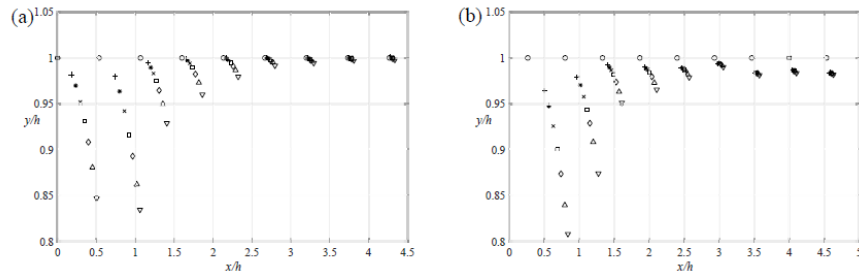


Figure 4. Time-averaged tip position with various incoming flow velocity: No incoming flow (o),  $Re_H = 1.8 \times 10^4$  (+),  $2.1 \times 10^4$  (\*),  $2.5 \times 10^4$  (x),  $2.8 \times 10^4$  ( $\square$ ),  $3.1 \times 10^4$  ( $\diamond$ ),  $3.4 \times 10^4$  ( $\Delta$ ),  $3.7 \times 10^4$  ( $\nabla$ ). (a) Central column and b) neighbor column in the staggered configuration.

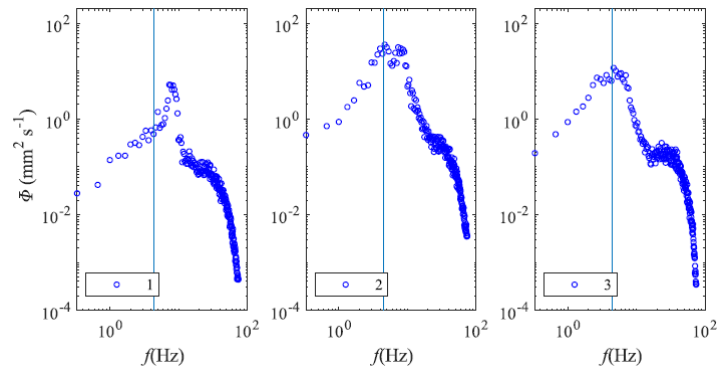


Figure 5. Example of the spectra of the tip velocity of selected canopy elements (1<sup>st</sup>, 2<sup>nd</sup> and 3<sup>rd</sup> rows).

## References

- Belcher, E. S. (2005) Mixing and transport in urban areas. *Phil. Trans. R. Soc. Lond. A* 363, 2947–2968.
- Dennison, W. C., Orth, R. J., Moore, K. A., Stevenson, J. C., Carter, V., Kollar, S., Bergstorm, P. W. and Batiuk, R. A. (1993) Assessing water quality with submersed aquatic vegetation. *BioScience* 43 (2), 86–94.
- Finnigan, J (2000) Turbulence in plat canopies. *Annu. Rev. Fluid Mech.* 2000. 32:519–571.
- Fonseca, M. S. and Cahalan, J. A. (1992) A preliminary evaluation of wave attenuation by four species of seagrass. *Estuar. Coast. Shelf Sci.* 35, 565–576.
- Hawkins, C. P., Murphy, M. L., Anderson, N. H. and Wilzbach, M. A. (1983) Density of fish and salamanders in relation to riparian canopy and physical habitat in streams of the northwestern United States. *Can. J. Fish. Aquat. Sci.* 40.
- Kim, J-T., Kim, D., Liberzon, A., and Chamorro, L. P. (2016) Three-dimensional particle tracking velocimetry for turbulence applications: Case of a jet flow. *Journal of visualized experiments: JoVE* (108).
- Luhar, M., and Nepf, H. M., (2016) Wave-induced dynamics of flexible blades. *Journal of Fluids and Structures*, 61, 20–41.
- Souch, C. and Grimmond, S. (2006) Applied climatology: urban climate. *Prog. Phys. Geog.* 30 (2), 270.